Molecular Crystals and Liquid Crystals

ISSN: 1542-1406 (Print) 1563-5287 (Online) Journal homepage: http://www.tandfonline.com/loi/gmcl20

A comparative analysis between conventional and new twelve sectors direct torque control strategies of induction machine using a multi level inverter

Mouna Essaadi, Mohamed Khafallah, Abdallah Saad & Abdelouahed El Hajjaji

To cite this article: Mouna Essaadi, Mohamed Khafallah, Abdallah Saad & Abdelouahed El Hajjaji (2016) A comparative analysis between conventional and new twelve sectors direct torque control strategies of induction machine using a multi level inverter, Molecular Crystals and Liquid Crystals, 628:1, 180-187, DOI: 10.1080/15421406.2015.1137266

To link to this article: http://dx.doi.org/10.1080/15421406.2015.1137266

Published online: 13 May 2016.

MOL. CRYST. LIQ. CRYST.
2016, VOL. 628, 180–187
http://dx.doi.org/10.1080/15421406.2015.1137266

Taylor & Francis
Taylor & Francis Group

A comparative analysis between conventional and new twelve sectors direct torque control strategies of induction machine using a multi level inverter

Mouna Essaadi[a], Mohamed Khafallah[a], Abdallah Saad[a], and Abdelouahed El Hajjaji

[a]Hassan II University-ENSEM, Oasis, Casablanca, Morocco; [b]Laboratory of Engineer Sciences for Energy (LabSIPE), National School of Applied Sciences, University Chouaib Doukkali, El Jadida, Morocco

ABSTRACT
this paper presents a comparative analysis between conventional twelve sectors direct torque control (12_DTC) and a new twelve sectors direct torque control (12_DTC_3L) using a neutral clamped point (NPC) three level inverter. Those different strategies are compared by simulation in term of torque, flux and stator current performances. Finally, a summary of the comparative analysis is presented.

KEYWORDS
12_DTC; 12_DTC_3L; NPC; torque dynamic; stator current; flux; performances

I. Introduction

Traditionally, variable speed electric machines were based on DC motors, since the magnetic flux and torque are easily controlled by the stator and rotor current, respectively [1]. For the last two decades, DC motors was replaced by AC motors. Induction Machine (IM) is one of the robust AC motors that have been widely used in industry. However, due to their highly coupled non-linear structure, a high performance control of IM is a challenging problem [2]. Field oriented control (FOC) has been till now employed in high performance industry applications using IM instead of DC motors. FOC of IM has achieved a quick torque response and has many similar advantages to DC motors. However, it depends to accurate parameter identification to achieve the expected performance [3] [1]. During the last decade, a new control method called Direct Torque Control (DTC) has been created. DTC is characterized by his simple implementation and robustness. However, DTC has some disadvantages compared with new DTC strategies, like 12_DTC. This method still the best DTC method in almost the majority of the performances studied [4]. In order to improve the 12_DTC to have better performances especially to reduce torque ripples, this paper give a comparative analysis between 12_DTC and 12_DTC_3L, in term of torque, flux and stator current performances based on simulation results.

II. Principle of 12_ dtc

Since M. Depenbrock and I. Takahashi proposed DTC for IM in the middle of 1980′s, more than decade has passed. It is getting more and more popular nowadays [5]. The instantaneous

CONTACT Mouna Essaadi mounaessaadi2@gmail.com
Color versions of one or more of the figures in the article can be found online at www.tandfonline.com/gmcl.

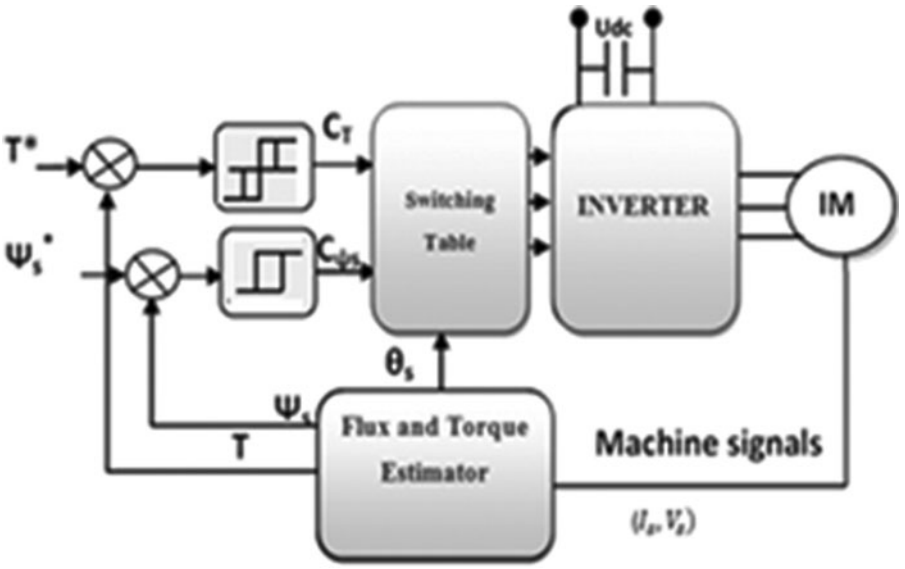

Figure 1. Block diagram of the DTC control technique.

values of the stator flux and torque are calculated from stator variable by using a closed loop estimator [6]. As shown in Fig. 1, stator flux and torque can be controlled directly and independently by properly selecting the inverter switching configuration [4].

By using an α-β stationary stator reference frame, the stator flux linkage ψ_s and electromagnetic torque are calculating by using:

$$\psi_s = \sqrt{{\psi_{\alpha s}}^2 + {\psi_{\beta s}}^2} \tag{1}$$

Where:

$$\psi_{\alpha s} = \int_0^t (\mathrm{V}_{\alpha s} - \mathrm{R}_s \mathrm{I}_{\alpha s}) dt \tag{2}$$

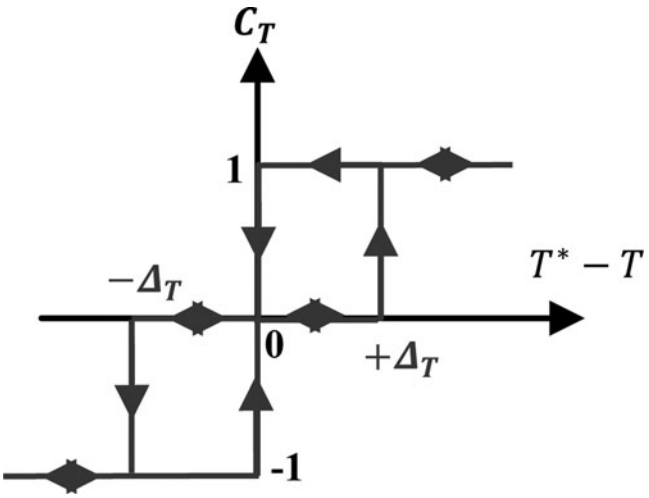

Figure 2. Torque hysteresis comparator.

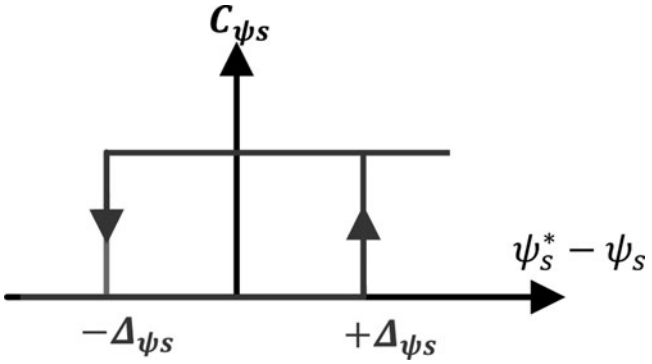

Figure 3. Flux hysteresis comparator.

$$\psi_{\beta s} = \int_0^t (\mathrm{V}_{\beta s} - \mathrm{R_s I}_{\beta s})dt \tag{3}$$

The angle θ_s is equal to:

$$\theta_s = \tan^{-1}\left(\frac{\psi_{\beta s}}{\psi_{\alpha s}}\right) \tag{4}$$

$$T = p\left[\psi_{\alpha s}\mathrm{I}_{\beta s} - \psi_{\beta s}\mathrm{I}_{\alpha s}\right] \tag{5}$$

The error between the estimated torque and the reference torque T* is the input of a three level hysteresis comparator, whereas the error between the estimated stator flux magnitude ψ_s and he reference stator flux magnitude ψ_s* is the input of a two level hysteresis comparator.

Figs. 2 and 3 illustrate the torque and flux comparators, respectively.

The selection of the appropriate voltage vector is based on the switching table given in Table 1. The input quantities are the flux sector and the outputs of the two hysteresis comparators.

To determine stator vector voltage to be applied, we begin by dividing the circular trajectory of the stator flux into six symmetrical sectors referred as the inverter voltage vectors [7].

Then, we study the effect of each stator voltage on the flux and torque. When the stator flux is in sector Si, the vectors V_{i+1}or V_{i-1} are selected to increase its amplitude, and V_{i+2}or V_{i-2} to decrease it. However V_{i+1}or V_{i+2} increase the torque and V_{i-1}or V_{i-2} decrease it. Fig. 4 shows the effect of those different choices in sector S1

In C_DTC there are two states per sector i that present a torque ambiguity which are $\bar{\mathrm{V}}_{\mathrm{i}}$ and$\bar{\mathrm{V}}_{\mathrm{i+1}}$. Therefore, they are never used. In a same way, in M_DTC there are two states per

Table 1. Basic switching.

Outputs of hysteresis comparators		Sector					
$C_{\psi S}$	C_{Te}	1	2	3	4	5	6
1	1	$\bar{V}_2$	$\bar{V}_3$	$\bar{V}_4$	$\bar{V}_5$	$\bar{V}_6$	$\bar{V}_1$
	0	$\bar{V}_7$	$\bar{V}_0$	$\bar{V}_7$	$\bar{V}_0$	$\bar{V}_7$	$\bar{V}_0$
	−1	$\bar{V}_6$	$\bar{V}_1$	$\bar{V}_2$	$\bar{V}_3$	$\bar{V}_4$	$\bar{V}_5$
0	1	$\bar{V}_3$	$\bar{V}_4$	$\bar{V}_5$	$\bar{V}_6$	$\bar{V}_1$	$\bar{V}_2$
	0	$\bar{V}_0$	$\bar{V}_7$	$\bar{V}_0$	$\bar{V}_7$	$\bar{V}_0$	$\bar{V}_7$
	−1	$\bar{V}_5$	$\bar{V}_6$	$\bar{V}_1$	$\bar{V}_2$	$\bar{V}_3$	$\bar{V}_4$

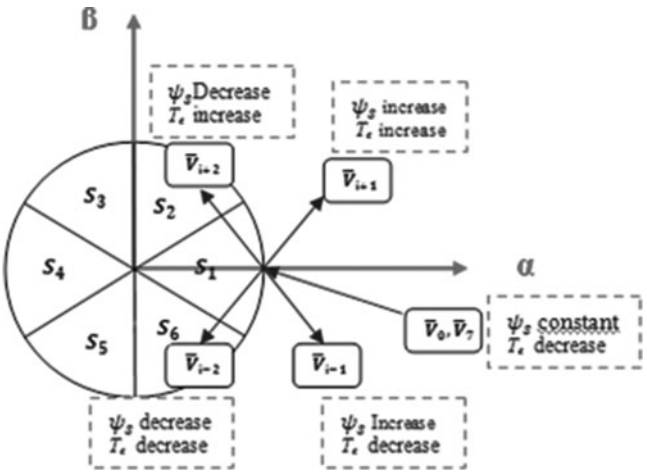

Figure 4. Effect of different Vs choices on the torque and stator flux in sector S1.

sector i that introduce flux ambiguity which are $\bar{V}_{i+2}$ and $\bar{V}_{i+5}$, so they are never used either. If the stator flux locus is divided into twelve sectors [8] instead of just six, all six active states will be used per sector and the problem of ambiguity of both flux and torque will be solved. This new stator flux locus is introduced in Fig. 5.

It's clearly noticed in Table 2 that all the six vectors are used disappearing all ambiguities.

Switching table of the 12_DTC becomes Table 5.As shown in Fig. 5, It is obvious that V1 will produce a large increase in flux and a small increase in torque in sector S12. On the contrary, V2 will increase the torque in large proportion and the flux in a small one. It is reasonable to deduce that the torque error should be divided in the number of intervals that later on will be measured.

III. Principle of three level NPC inverter

Multilevel inverter present a big interest in the field of the high voltages and the high powers of the fact that they introduce less distortion and weak losses with relatively low switching

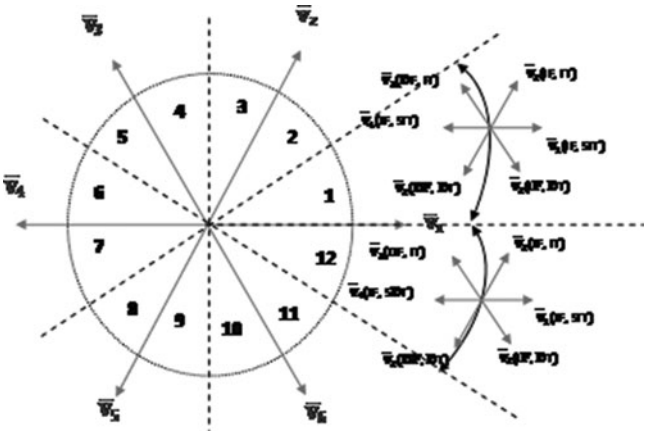

Figure 5. Twelve sectors modified DTC(12_DTC).IT/DT/IF/DC/SIT/SDT: Increase Torque/Decrease torque/ Increase flux/ decrease Flux/Small increase of Torque/Small decrease of torque.

Table 2. Switching table of the 12_DTC.

	Sector												
$C_{\psi S}$	C_{Te}	1	2	3	4	5	6	7	8	9	10	11	12
1	*2*	$\bar{V}_2$	$\bar{V}_3$	$\bar{V}_3$	$\bar{V}_4$	$\bar{V}_4$	$\bar{V}_5$	$\bar{V}_5$	$\bar{V}_6$	$\bar{V}_6$	$\bar{V}_1$	$\bar{V}_1$	$\bar{V}_2$
	1	$\bar{V}_2$	$\bar{V}_2$	$\bar{V}_3$	$\bar{V}_3$	$\bar{V}_4$	$\bar{V}_4$	$\bar{V}_5$	$\bar{V}_5$	$\bar{V}_6$	$\bar{V}_6$	$\bar{V}_1$	$\bar{V}_1$
	-1	$\bar{V}_1$	$\bar{V}_1$	$\bar{V}_2$	$\bar{V}_2$	$\bar{V}_3$	$\bar{V}_3$	$\bar{V}_4$	$\bar{V}_4$	$\bar{V}_5$	$\bar{V}_5$	$\bar{V}_6$	$\bar{V}_6$
	-2	$\bar{V}_6$	$\bar{V}_1$	$\bar{V}_1$	$\bar{V}_2$	$\bar{V}_2$	$\bar{V}_3$	$\bar{V}_3$	$\bar{V}_4$	$\bar{V}_4$	$\bar{V}_5$	$\bar{V}_5$	$\bar{V}_6$
0	*2*	$\bar{V}_3$	$\bar{V}_4$	$\bar{V}_4$	$\bar{V}_5$	$\bar{V}_5$	$\bar{V}_6$	$\bar{V}_6$	$\bar{V}_1$	$\bar{V}_1$	$\bar{V}_2$	$\bar{V}_2$	$\bar{V}_3$
	1	$\bar{V}_4$	$\bar{V}_4$	$\bar{V}_5$	$\bar{V}_5$	$\bar{V}_6$	$\bar{V}_6$	$\bar{V}_1$	$\bar{V}_1$	$\bar{V}_2$	$\bar{V}_2*$	$\bar{V}_3$	$\bar{V}_3$
	-1	$\bar{V}_7$	$\bar{V}_5$	$\bar{V}_0$	$\bar{V}_6$	$\bar{V}_7$	$\bar{V}_1$	$\bar{V}_0$	$\bar{V}_2$	$\bar{V}_7$	$\bar{V}_3$	$\bar{V}_0$	$\bar{V}_4$
	-2	$\bar{V}_5$	$\bar{V}_6$	$\bar{V}_6$	$\bar{V}_1$	$\bar{V}_1$	$\bar{V}_2$	$\bar{V}_2$	$\bar{V}_3$	$\bar{V}_3$	$\bar{V}_4$	$\bar{V}_4$	$\bar{V}_5$

frequency. The three-level inverters presented in Fig. 6 has several advantages over the standard two-level inverter, such as a greater number of levels in the waveforms, less harmonic distortion. [9]

The connexion function for each switch is defined [10]:

$$F_{ki} = \begin{cases} = 1 \text{ if switch is on} \\ = 0 \text{ if switch is off} \end{cases} \tag{6}$$

The relation between the four switches for each phase is is:

$$F_{k1} = 1 - F_{k4} \; ; \; F_{k2} = 1 - F_{k3} \tag{7}$$

With k = 1,2,3 is the phase number the half phase connexion function F_{km}^{b} is defined:

$$F_{k1}^{b} = F_{k1} X F_{k2} \; ; \; F_{k0}^{b} = F_{k3} X F_{k4} \tag{8}$$

With m = 1 for the top half phase, m = 0 for the bottom.

The three phases tensions are defined by:

$$\begin{aligned} V_{AM} &= F_{11}^{b} X U_{C1} - F_{10}^{b} X U_{C2} \\ V_{BM} &= F_{21}^{b} X U_{C1} - F_{20}^{b} X U_{C2} \\ V_{CM} &= F_{31}^{b} X U_{C1} - F_{30}^{b} X U_{C2} \end{aligned} \tag{9}$$

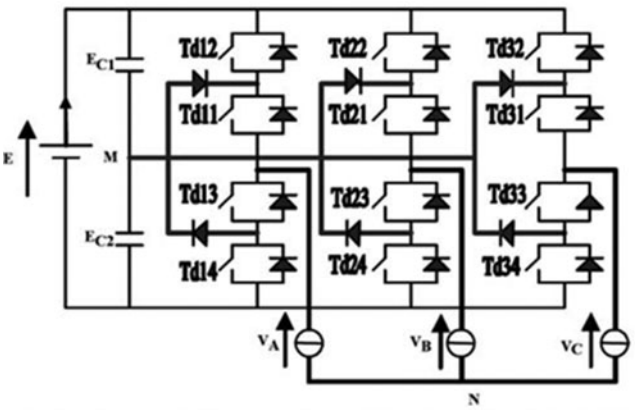

Figure 6. Three level inverter: NPC structure.

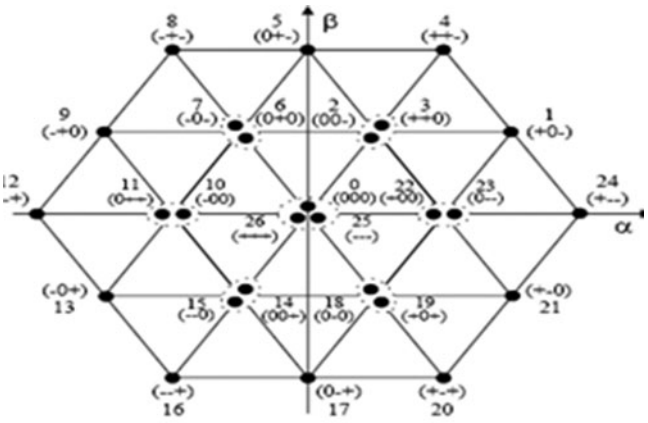

Figure 7. vectors tension generated by Three level inverter.

And then:

$$\begin{bmatrix} V_A \\ V_B \\ V_C \end{bmatrix} = \frac{1}{3}\begin{bmatrix} 2 & -1 & -1 \\ -1 & 2 & -1 \\ -1 & -1 & 2 \end{bmatrix} \times \left\{ \begin{bmatrix} F_{11}^b \\ F_{21}^b \\ F_{31}^b \end{bmatrix} U_{C1} - \begin{bmatrix} F_{10}^b \\ F_{20}^b \\ F_{30}^b \end{bmatrix} U_{C2} \right\} \tag{10}$$

with: $U_{C1} = U_{C2} = E/2$

The switching table of the 12_DTC_3L become Table 3

The following Fig. 7 shows the various discreet positions, in the plane, of the vector tension generated by the three levels inverter. [11]

IV. Simulation results and discussion

This section is aimed to give a contribution for a comparison between direct torque control methodologies (12_DTC and 12_DTC_3L).

The simulation has been carried out by using MATALAB SIMULINK on 1.5KW induction machine.

Fig. 8 presents the two DTC command: 12_DTC and 12_DTC_3L in term of Torque, flux and current performances. Fig. 8-a shows the two responses to a step change command from 0 N.m to 10 N.m at 0.0 s, the comparison between the two methods shows clearly that

Table 3. Switching table of the 12_DTC_3L.

	Sector												
$C_{\psi S}$	C_{Te}	1	2	3	4	5	6	7	8	9	10	11	12
1	*2*	$\bar{V}_{22}$	$\bar{V}_{17}$	$\bar{V}_{23}$	$\bar{V}_{18}$	$\bar{V}_{24}$	$\bar{V}_{0}$	$\bar{V}_{25}$	$\bar{V}_{20}$	$\bar{V}_{26}$	$\bar{V}_{15}$	$\bar{V}_{21}$	$\bar{V}_{16}$
	1	$\bar{V}_{2}$	$\bar{V}_{3}$	$\bar{V}_{10}$	$\bar{V}_{11}$	$\bar{V}_{4}$	$\bar{V}_{5}$	$\bar{V}_{12}$	$\bar{V}_{13}$	$\bar{V}_{6}$	$\bar{V}_{1}$	$\bar{V}_{8}$	$\bar{V}_{9}$
	-1	$\bar{V}_{13}$	$\bar{V}_{8}$	$\bar{V}_{1}$	$\bar{V}_{2}$	$\bar{V}_{9}$	$\bar{V}_{10}$	$\bar{V}_{3}$	$\bar{V}_{4}$	$\bar{V}_{11}$	$\bar{V}_{12}$	$\bar{V}_{5}$	$\bar{V}_{6}$
	-2	$\bar{V}_{20}$	$\bar{V}_{26}$	$\bar{V}_{15}$	$\bar{V}_{21}$	$\bar{V}_{16}$	$\bar{V}_{22}$	$\bar{V}_{17}$	$\bar{V}_{23}$	$\bar{V}_{18}$	$\bar{V}_{24}$	$\bar{V}_{19}$	$\bar{V}_{25}$
0	*2*	$\bar{V}_{17}$	$\bar{V}_{23}$	$\bar{V}_{18}$	$\bar{V}_{24}$	$\bar{V}_{19}$	$\bar{V}_{4}$	$\bar{V}_{20}$	$\bar{V}_{26}$	$\bar{V}_{15}$	$\bar{V}_{21}$	$\bar{V}_{16}$	$\bar{V}_{22}$
	1	$\bar{V}_{3}$	$\bar{V}_{4}$	$\bar{V}_{11}$	$\bar{V}_{12}$	$\bar{V}_{4}$	$\bar{V}_{2}$	$\bar{V}_{13}$	$\bar{V}_{8}$	$\bar{V}_{1}$	$\bar{V}_{2}$	$\bar{V}_{9}$	$\bar{V}_{10}$
	-1	$\bar{V}_{5}$	$\bar{V}_{6}$	$\bar{V}_{13}$	$\bar{V}_{8}$	$\bar{V}_{1}$	$\bar{V}_{2}$	$\bar{V}_{9}$	$\bar{V}_{10}$	$\bar{V}_{3}$	$\bar{V}_{4}$	$\bar{V}_{11}$	$\bar{V}_{12}$
	-2	$\bar{V}_{25}$	$\bar{V}_{20}$	$\bar{V}_{26}$	$\bar{V}_{15}$	$\bar{V}_{21}$	$\bar{V}_{16}$	$\bar{V}_{22}$	$\bar{V}_{17}$	$\bar{V}_{23}$	$\bar{V}_{18}$	$\bar{V}_{24}$	$\bar{V}_{19}$

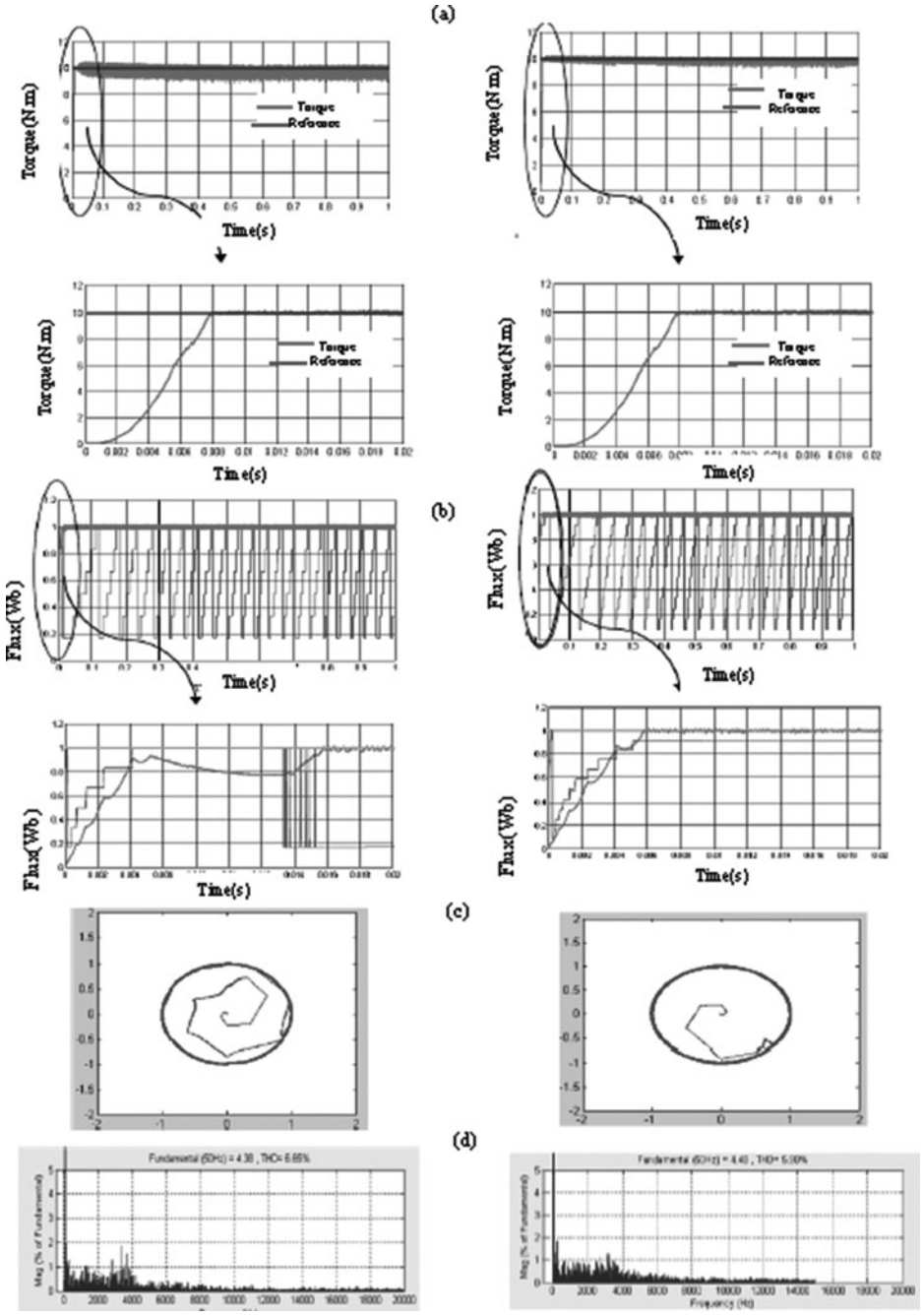

Figure 8. Comparison between: 12_DTC and 12_DTC_3L in term of (a) torque, (b) flux performances in steady state and transient conditions,(c) stator flux circle and(d) THD.

12_DTC_3L reduce remarkably torque ripples compared with 12_DTC, but both of the methods gives a good torque dynamic responses. Fig. 8-b shows the two flux responses to a flux reference equal to 1 Wb, in term of flux dynamic response, 12_DTC_3L give a very good performance comparing with 12_DTC, that means, trajectory of stator flux established more quickly than that of 12_DTC (Fig. 8-c). In term of steady state stator current distortions, the better performance is given by 12_DTC_3L by reducing the THD till 5.90% (Fig. 8-d). Table 4

Table 4. A comparative analysis between 12_DTC and 12_DTC_3L.

DTC control		
Performances	12_DTC	12_DTC_3L
Torque Dynamic response	Fast (8 ms)	Fast (8 ms)
Torque in steady state	ripples	Less ripples
Flux in steady state	More ripples	Less ripples
Stator current in steady state	Distortions (TDH = 6.65%)	Less distortions (TDH = 5.90%)
Switching frequency	Important (six sitches)	Less important (twelve switches)

gives a comparative analysis between 12_DTC and 12_DTC_3L in term of different performances studied before.

V. Conclusion

In this paper a comparative analysis between different DTC strategies have been presented. This work began by explaining the principle of The C_DTC, M_DTC and 12_DTC.The paper presents later a discussion based on the simulation results presented in the same work. It's clear that M_DTC still a very competitive DTC control compared with C_DTC and 12_DTC in term of Flux in both transient and steady state also in his simplicity of implementation, but M_DTC presents more ripples, in term of torque in steady state, and stator current distortions. 12_DTC still the best DTC method in almost the majority of the performances studied in this work. In order to improve the 12_DTC to have better performances, this method will be associated to a multilevel inverter in a future work.

References

[1] Ramya, R., Abhijith, A., Raju, S. H., Aditya Bhat, S. M., & Thilak, M. (2012). *Undergraduate Academic Research Journal (UARJ)*, *2*(3,4), 4–8.
[2] Chaikhy, H., Khafallah, M., Saad, A., & Es-saadi, M. (2011). *Canadian Journal on Electrical and Electronics Engineering*, *2*(7), 270–274.
[3] Toufouti, R., Meziane, S., & Benalla, H. (2007). *Journal of Theoretical and Applied Information Technology*, *3*(3), 35–44.
[4] Es-saadi, M., Khafallah, M., Saad, A., & Chaikhy, H. (2014). Second World Conference on Complex Systems (WCCS), IEEE, 350–354.
[5] Khafallah, M., Saad, A., & Chikh, K. (2011). *International Review on Modeling and Simulation (IREMOS)*, *4*(6), 2811–2816.
[6] Takahashi, I., & Noguchi, T. (1986). *IEEE Trans. On IA*, *22*(5), 820–827.
[7] Chaikhy, H., Khafallah, M., Saad, A., Es-saadi, M., & Chikh, K. (2011). *Revue de génie industriel*, *6*, 23–32.
[8] Mokhtari, B., Ameur, A., Benkhoris, M. F., Mokrani, L., & Azoui, B. (2012). International Conference on Renewable Energies and Power Quality (ICREPQ'12) Santiago de Compostela (Spain), March.
[9] Schibili, N., Nguyen, T., & Rufer, A. (1998). *IEEE Trans. On Power Elect*, *13*, 5.
[10] Abdelkrim, T., Berkouk, E.M., Aliouane, K., Benamrane, K., & Benslimane, T. (2011). *Revue des Energies Renouvelables*, *14*(2), 211–217.
[11] Ouboubker, L., Khafallah, M., Lamterkati, J., & Chikh, K. (2014). International Conference on Multimedia Computing and Systems (ICMCS), IEEE, 1051–1058.